OFDM Spread Spectrum with Index Modulation

Qiang Li[†,$], Miaowen Wen[†,$], Ertugrul Basar[‡], and Fangjiong Chen[†]
[†]School of Electronic and Information Engineering,
South China University of Technology, Guangzhou 510640, China
[$]National Mobile Communications Research Laboratory, Southeast University, Nanjing 210096, China
[‡]Faculty of Electrical and Electronics Engineering, Istanbul Technical University, Istanbul 34469, Turkey
Email: eeqiangli@mail.scut.edu.cn, {eemwwen, eefjchen}@scut.edu.cn, basarer@itu.edu.tr

***Abstract*— In this paper, we propose index modulated orthogonal frequency division multiplexing spread spectrum (IM-OFDM-SS) scheme, which combines the techniques of SS and IM under the framework of OFDM. In this scheme, the information bits are jointly conveyed by the indices of spreading codes and the conventional M-ary modulated symbols. A low-complexity maximum ratio combining (MRC) detector is designed, in which the receiver first detects the selected spreading codes and then the corresponding data symbols are de-spread and demodulated. The bit error probability (BEP) upper bound and the achievable diversity order are analyzed according to the union bounding technique. Simulation results verify the analyses and show that the proposed IM-OFDM-SS outperforms the existing OFDM-IM and OFDM-SS schemes significantly.**

I. Introduction

The concept of IM, which utilizes the index(es) of some transmission entities to carry extra information bits, has been proposed as a competitive alternative digital modulation technique for the future wireless communications [1]-[3], and it has attracted significant attention in recent times.

Inspired by the spatial modulation (SM), which considers an M-ary modulated symbol and the index of an active antenna as the information-bearing units [4], a number of researchers also applied the IM principle to OFDM subcarriers. In subcarrier-index modulation OFDM (SIM-OFDM) scheme [5], one index bit is offered to each subcarrier and the subcarriers with the majority bit-value are activated to transmit symbols. The number of active subcarriers in each OFDM block is variable and a perfect feedforward link is needed to signify the majority bit-value to the receiver, which make this scheme less practical. Enhanced (E-)SIM-OFDM avoids these drawbacks by employing one index bit to control the states of two consecutive subcarriers [6]. However, the spectral efficiency (SE) of ESIM-OFDM systems is far behind that of OFDM systems if the same constellation size is adopted. A more flexible and efficient IM scheme for OFDM named OFDM with IM (OFDM-IM) is proposed in [7], in which the total subcarriers are divided into several blocks and a subset of subcarriers within each block are activated according to the index bits to transmit M-ary modulated symbols.

The achievable performance of OFDM-IM in terms of bit error rate (BER) [7], minimum Euclidean distance [8], achievable rate [9], and inter-carrier interference [10] is analyzed, revealing the superiority of OFDM-IM over its OFDM counterpart. Due to the advantages of OFDM-IM, plenty of research studies on OFDM-IM and its variants have emerged. Apart from the maximum-likelihood (ML) detector, some low-complexity detectors, such as log-likelihood ratio detector [7], low-complexity ML detector [11] and greedy detector [12], are proposed to ease the computational burden on the receiver.

Based on the framework of OFDM-IM, some efforts to increase its SE and diversity order have been made in the literature. On the issue of SE, in multiple-input multiple-output (MIMO-)OFDM-IM scheme [13], [14], each transmit antenna is equipped with an OFDM-IM transmitter such that the SE increases with the number of transmit antennas. A generic IM scheme for MIMO-OFDM systems, called generalized space and frequency index modulation (GSFIM) is proposed in [15], performing IM in both space and frequency domains. In [16], the "inactive" subcarriers in conventional OFDM-IM are re-activated intentionally to transmit symbols drawn from a constellation different from that employed by the "active" subcarriers. This scheme, called dual-mode IM aided OFDM (DM-OFDM), increases the number of ordinary modulation bits, while keeping the number of index bits unchanged. More recently, the number of modes is relaxed by the scheme of multiple-mode (MM-)OFDM-IM [17], and the full permutation of modes are used to convey a higher number of index bits.

On the other hand, there already exist some enhanced schemes improving the asymptotic BER performance of OFDM-IM and related systems. In [18], the subcarrier-level interleaving is introduced into OFDM-IM to obtain frequency diversity. In coordinate interleaved OFDM-IM (CI-OFDM-IM) [19], the real and imaginary parts of each complex data symbol are transmitted on two different active subcarriers using the CI orthogonal design, which increases the transmit diversity order of ordinary modulation bits from unity to two. To increase the transmit diversity order of index bits solely, the same index bits are fed into two or more blocks in [20]. In [21], the linear constellation precoded OFDM-IQ-IM (LP-OFDM-IQ-IM) is designed, in which an additional diversity gain is harvested through linear constellation precoding. Space-frequency code is constructed in [22] to improve the transmit diversity of MIMO-OFDM-IM.

Spread spectrum (SS) signals are widely used for the transmission of digital information over some radio channels, to offer code division multiple access (CDMA), message privacy, and the capability of combating the determined interference.

The combination of OFDM and SS, termed OFDM-SS in single-user communications and multi-carrier (MC-)CDMA in multi-user communications, is the attempt to exploit the advantages of both OFDM and SS [23].

Against the background, this paper proposes a novel IM scheme, termed IM-OFDM-SS, aiming at improving the diversity order of OFDM-IM and the SE of OFDM-SS. In IM-OFDM-SS, a data symbol is spread across several subcarriers to harvest additional diversity gain by the spreading code that is selected from a predefined set according to the index bits. The contributions of this paper are summarized as follows:

- The techniques of IM and SS are combined under the framework of OFDM in the IM-OFDM-SS scheme. To the best of our knowledge, IM for OFDM-SS has not been studied yet in the literature and the code IM is only proposed previously in the time-domain for direct sequence SS communications [24], [25].
- Taking into account the channel estimation errors, the ML and low-complexity near-optimum MRC detectors are proposed for IM-OFDM-SS. We derive an upper bound on the BEP of IM-OFDM-SS assuming ML detection, from which the diversity order is obtained.
- Extensive computer simulations are performed, whose results show that IM-OFDM-SS outperforms the existing OFDM, OFDM-IM, and OFDM-SS schemes significantly.

Notation: Column vectors and matrices are denoted by lowercase and capital bold letters, respectively. Superscripts *, ^{T}, and ^{H} stand for conjugate, transpose, and Hermitian transpose, respectively. $\mathbb{C}$ denotes the ring of complex numbers. $\det(\cdot)$ and $\mathrm{rank}(\cdot)$ return the determinant and rank of a matrix, respectively. $\mathrm{diag}(\cdot)$ transforms a vector into a diagonal matrix. $\mathcal{CN}(0,\sigma^2)$ represents the complex Gaussian distribution with zero mean and variance σ^2. The probability of an event and the probability density function (PDF) are denoted by $\Pr(\cdot)$ and $f(\cdot)$, respectively. $Q(\cdot)$ is the Gaussian Q-function. $\mathbf{I}_n$ is the $n\times n$ identity matrix. $C(\cdot,\cdot)$ and $\|\cdot\|$ denote the binomial coefficient and the Frobenius norm, respectively. We define $[x_1,\ldots,x_n]^T\otimes[y_1,\ldots,y_n]^T=[x_1y_1,\ldots,x_ny_n]^T$.

II. System Model

In this section, we present the transmitter and receiver structures of IM-OFDM-SS.

A. Transmitter

The transmitter structure of IM-OFDM-SS based on the framework of OFDM with N subcarriers is depicted in Fig. 1. To perform IM efficiently, m information bits to be sent for each OFDM frame duration are equally separated into g blocks and IM is performed within $n=N/g$ subcarriers in a block-wise manner. Since the processes in all blocks are the same and independent of each other, let us take the β-th block as an example, where $\beta\in\{1,\ldots,g\}$. In the β-th block, the available $p=m/g$ bits are further divided into two parts. The first part consisting of p_1 index bits are used to select the spreading code $\mathbf{c}_{i^{(\beta)}}\in\mathbb{C}^{n\times 1}$ from a predefined set $\mathcal{C}=\{\mathbf{c}_1,\ldots,\mathbf{c}_n\}$, where $i^{(\beta)}\in\{1,\ldots,n\}$ is the index of the spreading code for the β-th block. The second part with $p_2=\log_2(M)$ symbol bits are mapped into a symbol $s^{(\beta)}\in\mathcal{X}$, where $\mathcal{X}$ is an M-ary phase shift keying (PSK)/quadrature amplitude modulation (QAM) constellation having unit average power.

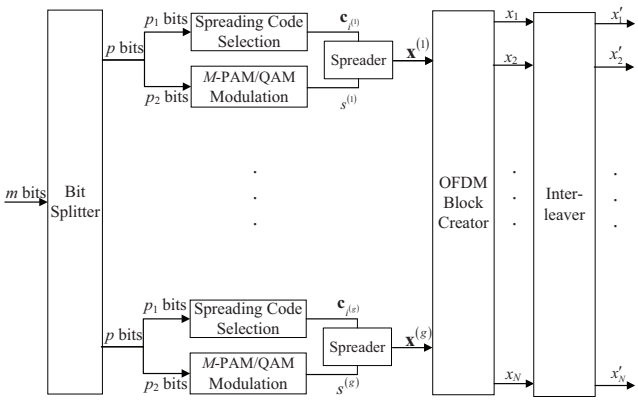

Fig. 1. Transmitter structure of IM-OFDM-SS.

To enable low-complexity detection at the receiver, the spreading codes in $\mathcal{C}$ should be mutually orthogonal. In this paper, Zadoff-Chu and Walsh codes are considered [26]. Due to the length constraint of Walsh codes, n is assumed to be an integer power of 2. Therefore, we set $p_1=\log_2(n)$ and the mapping and de-mapping between p_1 bits and $i^{(\beta)}$ can be easily implemented by the natural binary code [27].

Then, the symbol $s^{(\beta)}$ is spread across n subcarriers by the selected spreading code $\mathbf{c}_{i^{(\beta)}}$, yielding

$$\begin{aligned}\mathbf{x}^{(\beta)}&=\left[x_1^{(\beta)},\ldots,x_n^{(\beta)}\right]^T=s^{(\beta)}\mathbf{c}_{i^{(\beta)}}\\&=\left[s^{(\beta)}c_{i^{(\beta)},1},\ldots,s^{(\beta)}c_{i^{(\beta)},n}\right]^T,\end{aligned}\tag{1}$$

where $c_{i^{(\beta)},k},k\in\{1,\ldots,n\}$ is the k-th element of $\mathbf{c}_{i^{(\beta)}}$. After obtaining and concatenating $\mathbf{x}^{(\beta)}$ for all β, we obtain the $N\times 1$ main OFDM block as follows:

$$\begin{aligned}\mathbf{x}_F=[x_1,\ldots,x_N]^T&=\left[\left(\mathbf{x}^{(1)}\right)^T,\ldots,\left(\mathbf{x}^{(g)}\right)^T\right]^T\\&=\left[x_1^{(1)},\ldots,x_n^{(1)},x_1^{(2)},\ldots,x_n^{(2)},\ldots,x_1^{(g)},\ldots,x_n^{(g)}\right]^T.\end{aligned}\tag{2}$$

To harvest the frequency diversity, an interleaver is adopted, which makes the symbols in the $\mathbf{x}^{(\beta)}$ spaced equally by g subcarriers, obtaining

$$\begin{aligned}\mathbf{x}'_F&=[x'_1,\ldots,x'_N]^T\\&=\left[x_1^{(1)},\ldots,x_1^{(g)},x_2^{(1)},\ldots,x_2^{(g)},\ldots,x_n^{(1)},\ldots,x_n^{(g)}\right]^T.\end{aligned}\tag{3}$$

Afterwards, the remaining procedures are the same as those of classical OFDM, which are omitted in Fig. 1. First, $\mathbf{x}'_F$

is processed by the inverse fast Fourier transform (IFFT), yielding the time-domain OFDM block

$$\mathbf{x}_T = [X_1, \ldots, X_N]^T = \frac{1}{\sqrt{N}} \mathbf{W}_N^H \mathbf{x}'_F, \tag{4}$$

where $\mathbf{W}_N$ is the $N \times N$ discrete Fourier transform (DFT) matrix with $\mathbf{W}_N^H \mathbf{W}_N = N\mathbf{I}_N$. An L-length cyclic prefix (CP) $[X_{N-L+1}, \ldots, X_N]^T$ is added to the beginning of $\mathbf{x}_T$. After the parallel-to-serial and digital-to-analog conversions, the data is transmitted over the frequency-selective Rayleigh fading channel, whose impulse response is given by $\mathbf{h}_T = [h_{T,1}, \ldots, h_{T,v}]^T$, where each entry of $\mathbf{h}_T$ is a circularly symmetric complex Gaussian random variable following the distribution $\mathcal{CN}(0, 1/v)$. Note that L is chosen to be larger than v to combat the intersymbol interference.

At the receiver, N-point FFT and de-interleaving are carried out in sequence after discarding the CP of the received signal. Hence, the input-output relationship in the frequency-domain for the β-th block is given by

$$\mathbf{y}^{(\beta)} = \mathbf{X}^{(\beta)} \mathbf{h}^{(\beta)} + \mathbf{w}^{(\beta)}, \tag{5}$$

where $\mathbf{X}^{(\beta)} = \text{diag}(\mathbf{x}^{(\beta)})$, $\mathbf{h}^{(\beta)}$ is the $n \times 1$ frequency-domain channel vector, and $\mathbf{w}^{(\beta)} \in \mathbb{C}^{n \times 1}$ is the noise vector in the frequency-domain with the distribution $\mathcal{CN}(\mathbf{0}, N_0 \mathbf{I}_n)$, With de-interleaving, the elements of $\mathbf{h}^{(\beta)}$ can be viewed as independent and identically distributed (i.i.d.), which means $\mathbf{h}^{(\beta)} \sim \mathcal{CN}(\mathbf{0}, \mathbf{I}_n)$. We rewrite (5) in a scalar form as

$$y_k^{(\beta)} = s^{(\beta)} h_k^{(\beta)} c_{i^{(\beta)},k} + w_k^{(\beta)}, k = 1, \ldots, n, \tag{6}$$

where $y_k^{(\beta)}$, $h_k^{(\beta)}$, and $w_k^{(\beta)}$ are the samples of $\mathbf{y}^{(\beta)}$, $\mathbf{h}^{(\beta)}$, and $\mathbf{w}^{(\beta)}$, respectively, at the k-th subcarrier. We define the average SNR per subcarrier as $\gamma = 1/N_0$. The SE of IM-OFDM-SS scheme regardless of the CP overhead is given by (bps/Hz)

$$\mathcal{E}_{\text{IM-OFDM-SS}} = (p_1 + p_2)/n = \log_2 (Mn)/n, \tag{7}$$

while the SE of OFDM-SS is $\mathcal{E}_{\text{OFDM-SS}} = \log_2 (M)/n$, from which we observe that IM-OFDM-SS achieves a higher SE than OFDM-SS.

B. Receiver

In this subsection, we address the detection problem of IM-OFDM-SS by taking into account the effects of channel estimation errors. Two different types of detectors are provided for the IM-OFDM-SS scheme, including the ML detector and the MRC detector. Since the encoding processes for all blocks are identical and independent, the detection can be performed block by block, and for brevity, in the sequel we only focus on one block and omit the superscript (β).

In practical systems, the channel vector $\mathbf{h}$ is estimated at the receiver as [28], [29]

$$\bar{\mathbf{h}} = \mathbf{h} + \mathbf{h}_e, \tag{8}$$

where $\mathbf{h}_e \in \mathbb{C}^{n \times 1}$ represents the vector of channel estimation errors with the distribution $\mathcal{CN}(\mathbf{0}, \sigma_e^2 \mathbf{I}_n)$, and is independent of $\mathbf{h}$. Hence, $\bar{\mathbf{h}}$, whose elements are $\bar{h}_k, k = 1, \ldots, n$, follows the distribution $\mathcal{CN}(\mathbf{0}, (1 + \sigma_e^2)\mathbf{I}_n)$.

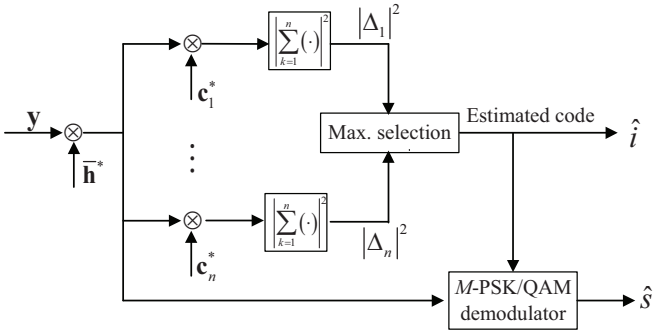

Fig. 2. MRC detector for IM-OFDM-SS.

1) ML detector: From (5), the mismatched ML detector makes a joint decision on the index of spreading code and the constellation symbol by searching all possible combinations of them, namely

$$(\hat{i}, \hat{s}) = \arg \min_{i,s} \left\| \mathbf{y} - \mathbf{X}\bar{\mathbf{h}} \right\|^2. \tag{9}$$

Then, the corresponding p information bits can be readily recovered from $\hat{i}$ and $\hat{s}$. Obviously, the computational complexity of the optimal ML detector in (9) in terms of complex multiplications is of order $\sim \mathcal{O}(Mn)$ per block.

2) MRC detector: In this detector, the detection process is divided into two steps, as described in Fig. 2. The first step is to estimate the selected spreading code, and the second step is to detect the information symbol based on the spreading code estimated in the first step.

At the first stage, $\mathbf{y}$ is fed into n one-tap equalizers in parallel, each of which is simply realized by one complex-valued multiplication per subcarrier. According to MRC, the l-th equalizer for the k-th subcarrier is given by $z_{l,k} = \bar{h}_k^* c_{l,k}^*$, and combining n subcarriers, yields

$$\Delta_l = \sum_{k=1}^{n} z_{l,k} y_k, \quad l = 1, \ldots, n. \tag{10}$$

Then, the squared values of the outputs of n branches are compared to determine the index of the selected spreading code via

$$\hat{i} = \arg \max_{l} |\Delta_l|^2. \tag{11}$$

After obtaining $\hat{i}$, at the second stage, the information symbol s can be estimated readily via

$$\hat{s} = \arg \min_{s} \left| \sum_{k=1}^{n} z_{\hat{i},k} y_k - s \sum_{k=1}^{n} \left| \bar{h}_k \right|^2 \right|^2. \tag{12}$$

From the description above, the computational complexity is of order $\sim \mathcal{O}(n + M)$, which is much lower than that of ML detector.

III. BEP Upper Bound And Diversity Order Analyses

In this section, we derive an upper bound on the BEP of IM-OFDM-SS assuming ML detection in the presence of channel

estimation errors. Then, the diversity order achieved by IM-OFDM-SS is analyzed.

In the presence of channel estimation errors, the conditional pairwise error probability (PEP) can be calculated as [7]

$$\Pr\left(\mathbf{X}\to\hat{\mathbf{X}}\,|\bar{\mathbf{h}}\right) = Q\left(\frac{\left\|\left(\mathbf{X}-\hat{\mathbf{X}}\right)\bar{\mathbf{h}}\right\|^2}{\sqrt{2\sigma_e^2\left\|\mathbf{X}^H\left(\mathbf{X}-\hat{\mathbf{X}}\right)\bar{\mathbf{h}}\right\|^2+2N_0\left\|\left(\mathbf{X}-\hat{\mathbf{X}}\right)\bar{\mathbf{h}}\right\|^2}}\right), \tag{13}$$

where $\hat{\mathbf{X}}$ is the estimate of $\mathbf{X}$. Since $|c_{i,k}|^2=1$ for any $i,k\in\{1,\ldots,n\}$, we have

$$\begin{aligned}\left\|\mathbf{X}^H(\mathbf{X}-\hat{\mathbf{X}})\bar{\mathbf{h}}\right\|^2 &= \sum_{k=1}^{n}|sc_{i,k}|^2|(x_k-\hat{x}_k)\,\bar{h}_k|^2\\ &= \frac{1}{n}\|\mathbf{x}\|^2\left\|(\mathbf{X}-\hat{\mathbf{X}})\bar{\mathbf{h}}\right\|^2.\end{aligned} \tag{14}$$

Hence, (13) can be expressed as

$$\Pr\left(\mathbf{X}\to\hat{\mathbf{X}}\,|\bar{\mathbf{h}}\right) = Q\left(\sqrt{\frac{\left\|\left(\mathbf{X}-\hat{\mathbf{X}}\right)\bar{\mathbf{h}}\right\|^2}{2N_0+2\sigma_e^2\|\mathbf{x}\|^2/n}}\right). \tag{15}$$

By following the method presented in [7], we obtain an approximate unconditional PEP

$$\Pr\left(\mathbf{X}\to\hat{\mathbf{X}}\right)\approx\frac{1/12}{\det\left(\mathbf{I}_n+q_1\bar{\mathbf{K}}_n\mathbf{A}\right)}+\frac{1/4}{\det\left(\mathbf{I}_n+q_2\bar{\mathbf{K}}_n\mathbf{A}\right)}, \tag{16}$$

where $q_1=n/(4nN_0+4\|\mathbf{x}\|^2\sigma_e^2)$, $q_2=n/(3nN_0+3\|\mathbf{x}\|^2\sigma_e^2)$, and $\mathbf{A}=(\mathbf{X}-\hat{\mathbf{X}})^H(\mathbf{X}-\hat{\mathbf{X}})$. Then, According to the union bounding technique, a BEP upper bound can be given by

$$P_u\le\frac{1}{p2^p}\sum_{\mathbf{X}}\sum_{\hat{\mathbf{X}}}\Pr\left(\mathbf{X}\to\hat{\mathbf{X}}\right)N\left(\mathbf{X},\hat{\mathbf{X}}\right), \tag{17}$$

where $N(\mathbf{X},\hat{\mathbf{X}})$ is the number of erroneous bits when $\mathbf{X}$ is detected as $\hat{\mathbf{X}}$.

At high SNR, (17) approximates to

$$P_u\approx\frac{1}{p2^p}\sum_{\mathbf{X},\hat{\mathbf{X}}}\left(\prod_{\omega=1}^{d}\lambda_\omega\left(\bar{\mathbf{K}}_n\mathbf{A}\right)\right)^{-1}\times\left(\frac{1}{12q_1^d}+\frac{1}{4q_2^d}\right)N\left(\mathbf{X},\hat{\mathbf{X}}\right), \tag{18}$$

where $d=\mathrm{rank}(\bar{\mathbf{K}}_n\mathbf{A})=\mathrm{rank}(\mathbf{A})$ and $\lambda_\omega(\bar{\mathbf{K}}_n\mathbf{A}),\omega=1,\ldots,d$, are the nonzero eigenvalues of $\bar{\mathbf{K}}_n\mathbf{A}$.

Remark: The diversity order achieved by IM-OFDM-SS is given by $d_{\min}=\min\,\mathrm{rank}\,(\mathbf{A})$. Recalling that $\mathbf{A}=(\mathbf{X}-\hat{\mathbf{X}})^H(\mathbf{X}-\hat{\mathbf{X}})$, it can be found that $d_{\min}=n/2, n\ge 2$, when the transmitted spreading code is detected erroneously by the receiver. It is worth noting that we have $d=n$ when the receiver correctly detects the spreading code index and makes a decision error for the M-ary symbol. Compared with classical OFDM and OFDM-IM, a higher diversity order is obtained by IM-OFDM-SS when $n\ge 4$. Additionally, IM-OFDM-SS provides a flexible trade-off between the SE and the diversity order by adjusting n.

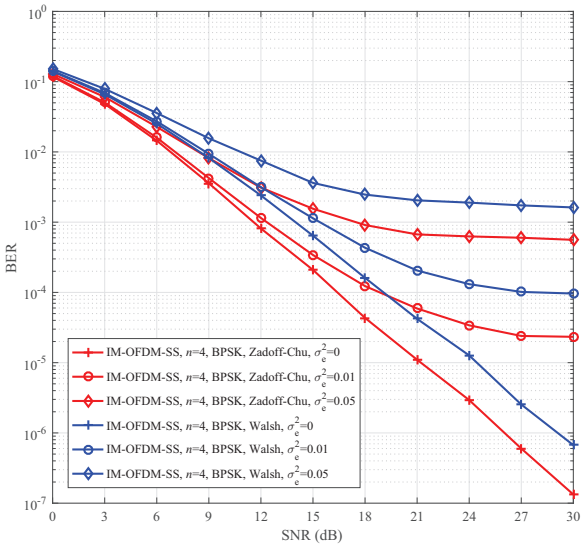

Fig. 3. Performance comparison between Zadoff-Chu and Walsh codes of IM-OFDM-SS with ML detectors (n=4, BPSK, $\sigma_e^2=0/0.01/0.05$).

IV. Simulation Results and Comparisons

In this section, the uncoded BER performance of IM-OFDM-SS over Rayleigh fading channels is evaluated through Monte Carlo simulations. To show the superiority of the proposed IM-OFDM-SS scheme, it is compared with classical OFDM, OFDM-IM [7], DM-OFDM [16], MM-OFDM-IM [17], CI-OFDM-IM [19], and OFDM-SS [23]. It is worth noting that the primary and the secondary constellations used by DM-OFDM are designed through constellation rotation. For simplicity, we will refer to "(CI-)OFDM-IM (n,k)" as the (CI-)OFDM-IM scheme in which k out of n subcarriers are active, and "DM-OFDM (n,k)" as the DM-OFDM scheme in which k out of n subcarriers are modulated by the primary constellation while the remaining subcarriers employ the secondary constellation.

To see the effects of different spreading codes, in Fig. 3, we present the BER curves of IM-OFDM-SS schemes with Zadoff-Chu and Walsh codes, where ML detectors, $n=4$, and BPSK are employed with $\sigma_e^2=0/0.01/0.05$. As seen from Fig. 3, the IM-OFDM-SS schemes with Zadoff-Chu codes outperform those with Walsh codes for $\sigma_e^2=0/0.01/0.05$ throughout the considered SNR region, which can be explained by the fact that IM-OFDM-SS schemes with Zadoff-Chu codes have larger minimum Euclidean distances between transmission vectors. In particular, we observe that without channel estimation errors, about 3dB SNR gain at a BER value of 10^{-5} can be achieved by the scheme with Zadoff-Chu codes compared with the scheme using Walsh codes; however,

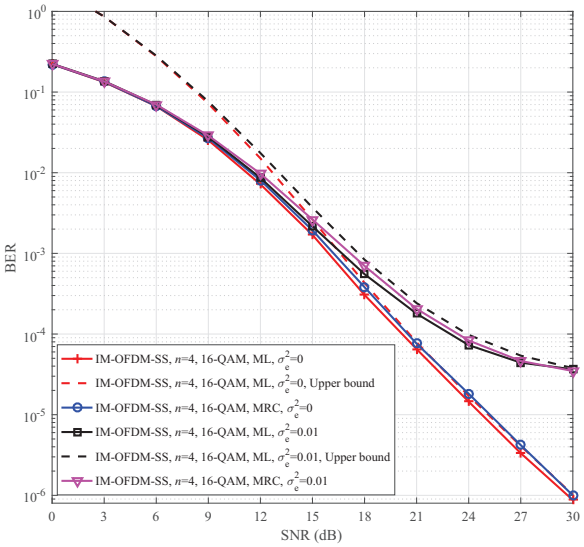

Fig. 4. Performance comparison between ML and MRC detectors of IM-OFDM-SS ($n = 4$, 16-QAM, $\sigma_e^2 = 0/0.01$).

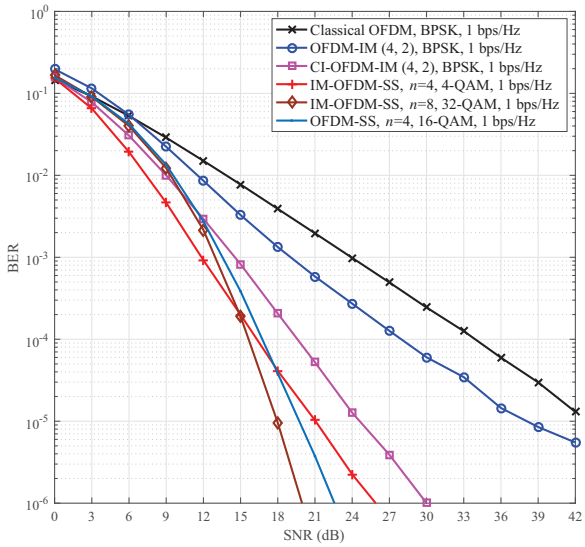

Fig. 5. Performance comparison among IM-OFDM-SS, classical OFDM, OFDM-IM, CI-OFDM-IM, and OFDM-SS at an SE of 1 bps/Hz. ML detectors are used for all schemes.

both of them have the same diversity order of two. The channel estimation errors deteriorate the performance greatly and error floors are observed in the high SNR region due to the mismatched ML detectors. However, the error floors with Zadoff-Chu codes are lower than those with Walsh codes. In addition, Zadoff-Chu codes result in the lower peak-to-average power ratio [23]. Due to these advantages, Zadoff-Chu codes are adopted in the rest of computer simulations.

Fig. 4 presents the performance comparisons between ML and MRC detectors of IM-OFDM-SS, where $n = 4$ and 16-QAM are employed with $\sigma_e^2 = 0/0.01$. To verify the analysis given in Section III, in the figures, we also plot the BEP upper bounds (17) for ML detectors. It can be observed from Fig. 4 that MRC detectors exhibit near-ML performance with/without channel estimation errors. For $\sigma_e^2 = 0$, both detectors achieve the same diversity order and less than 1dB SNR loss is incurred by the MRC detector compared with the ML detector. Besides, the BEP upper bounds become tight in the high SNR region, no matter whether there exist channel estimation errors or not.

In Figs. 5–6, the BER performance of ML detection of IM-OFDM-SS without channel estimation errors is evaluated at different SEs. In Fig. 5, we compare the BER performance of IM-OFDM-SS with $n = 4$ (8) and 4-QAM (32-QAM), classical OFDM with BPSK, OFDM-IM with $(n, k) = (4, 2)$ and BPSK, CI-OFDM-IM with $(n, k) = (4, 2)$ and BPSK, and OFDM-SS with $n = 4$ and 16-QAM at an SE of 1 bps/Hz. All schemes employ ML detectors. From Fig. 5, we observe that IM-OFDM-SS with $n = 8$ and 32-QAM, OFDM-SS, IM-OFDM-SS with $n = 4$ and 4-QAM, CI-OFDM-IM, OFDM-IM, and classical OFDM achieve diversity orders of 4, 4, 2, 2, 1, and 1, respectively. Both IM-OFDM-SS schemes perform better than classical OFDM, OFDM-IM, and CI-OFDM-IM for all SNR values. More specifically, in spite of the same diversity order, IM-OFDM-SS with $n = 4$ and 4-QAM obtains approximately 3dB SNR gain at a BER value of 10^{-5} over CI-OFDM-IM. Furthermore, IM-OFDM-SS with $n = 8$ and 32-QAM outperforms OFDM-SS throughout the considered SNR region and performs better than that with $n = 4$ and 4-QAM at high SNR due to its higher diversity order. Contrarily, because of the larger constellation size, IM-OFDM-SS with $n = 8$ and 32-QAM exhibits a worse BER than that with $n = 4$ and 4-QAM in the low SNR region.

The BER performance of IM-OFDM-SS with $n = 4$ and 64-QAM, classical OFDM with 4-QAM, OFDM-IM with $(n, k) = (4, 3)$ and 4-QAM, DM-OFDM with $(n, k) = (4, 2)$ and BPSK, MM-OFDM-IM with $n = 4$ and BPSK, CI-OFDM-IM with $(n, k) = (8, 6)$ and 4-QAM, and OFDM-SS with $n = 4$ and 256-QAM at an SE level of 1.5–2 bps/Hz is compared in Fig. 6. ML detectors are used for all schemes and an SE of 2 bps/Hz is achieved except DM-OFDM, which has an SE of 1.5 bps/Hz. Similar to the observations in Fig. 5, IM-OFDM-SS and CI-OFDM-IM achieve a higher diversity order than classical OFDM, OFDM-IM, DM-OFDM, and MM-OFDM-IM. Approximately 3dB SNR gain can be obtained at a BER value of 10^{-5} by IM-OFDM-SS compared with CI-OFDM-IM. Furthermore, in spite of a lower diversity order, IM-OFDM-SS performs better than OFDM-SS in the considered SNR region.

V. Conclusion

In this paper, we have proposed IM-OFDM-SS, in which the techniques of SS and IM are combined based on the framework of OFDM to improve the performance of existing OFDM, OFDM-IM, and OFDM-SS schemes. IM-OFDM-SS

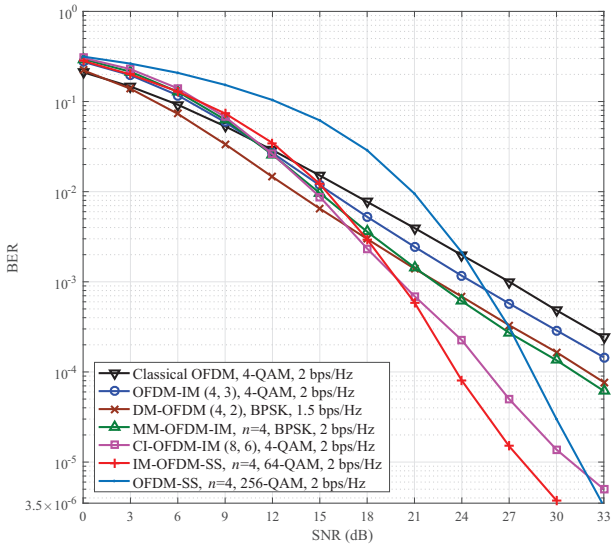

Fig. 6. Performance comparison among IM-OFDM-SS, classical OFDM, OFDM-IM, DM-OFDM, MM-OFDM-IM, CI-OFDM-IM, and OFDM-SS at an SE level of 1.5–2 bps/Hz. ML detectors are used for all schemes.

spreads an M-ary modulated symbol over several subcarriers by a spreading code and utilizes the index of the selected spreading code to convey additional bits. A low-complexity MRC-based detector has been designed for IM-OFDM-SS. An upper bound on the BEP has been derived, taking into account the channel estimation errors. Finally, the BER performance of IM-OFDM-SS has been simulated extensively, whose results show that IM-OFDM-SS significantly outperforms classical OFDM as well as the existing OFDM-IM and OFDM-SS schemes.

ACKNOWLEDGEMENT

This work was supported in part by the National Natural Science Foundation of China under Grant 61671211 and Grant 61501190, in part by the Natural Science Foundation of Guangdong Province under Grant 2016A030311024, in part by the State Major Science and Technology Special Projects under Grant 2016ZX03001009 and Grant 2017ZX03001001, and in part by the open research fund of National Mobile Communications Research Laboratory, Southeast University under Grant 2017D08.

REFERENCES

[1] M. Wen, X. Cheng, and L. Yang, *Index Modulation for 5G Wireless Communications*. Berlin, Germany: Springer, 2017.

[2] E. Basar, "Index modulation techniques for 5G wireless networks," *IEEE Commun. Mag.*, vol. 54, no. 7, pp. 168–175, July 2016.

[3] E. Basar, M. Wen, R. Mesleh, M. Di Renzo, Y. Xiao, and H. Haas, "Index modulation techniques for next-generation wireless networks," *IEEE Access*, vol. 5, pp. 16693–16746, 2017.

[4] P. Yang, M. Di Renzo, Y. Xiao, S. Li, and L. Hanzo, "Design guidelines for spatial modulation," *IEEE Commun. Surveys & Tuts.*, vol. 17, no. 1, pp. 6–26, First Quarter 2015.

[5] R. Abualhiga and H. Haas, "Subcarrier-index modulation OFDM," in *Proc. IEEE 20th Int. Symp. Pers., Indoor Mobile Radio Commun. (PIMRC)*, Tokyo, Japan, Sept. 2009, pp. 177–181.

[6] D. Tsonev, S. Sinanovic, and H. Haas, "Enhanced subcarrier index modulation (SIM) OFDM," in *Proc. IEEE Global Commun. Conf. (GLOBECOM) Workshops*, Houston, TX, USA, Dec. 2011, pp. 728–732.

[7] E. Basar, U. Aygolu, E. Panayirci, and H. V. Poor, "Orthogonal frequency division multiplexing with index modulation," *IEEE Trans. Signal Process.*, vol. 61, no. 22, pp. 5536–5549, Nov. 2013.

[8] N. Ishikawa, S. Sugiura, and L. Hanzo, "Subcarrier-index modulation aided OFDM - Will it work?," *IEEE Access*, vol. 4, pp. 2580–2593, 2016.

[9] M. Wen, X. Cheng, M. Ma, B. Jiao, and H. V. Poor, "On the achievable rate of OFDM with index modulation," *IEEE Trans. Signal Process.*, vol. 64, no. 8, pp. 1919–1932, Apr. 2016.

[10] Q. Ma, P. Yang, Y. Xiao, H. Bai, and S. Li, "Error probability analysis of OFDM-IM with carrier frequency offset," *IEEE Commun. Lett.*, vol. 20, no. 12, pp. 2434–2437, Dec. 2016.

[11] B. Zheng, F. Chen, M. Wen, F. Ji, H. Yu, and Y. Liu, "Low-complexity ML detector and performance analysis for OFDM with in-phase/quadrature index modulation," *IEEE Commun. Lett.*, vol. 19, no. 11, pp. 1893–1896, Nov. 2015.

[12] J. Crawford and Y. Ko, "Low complexity greedy detection method with generalized multicarrier index keying OFDM," in *Proc. IEEE 26th Annu. Int. Symp. Pers., Indoor, Mobile Radio Commun.*, Hong Kong, China, Aug. 2015, pp. 688–693.

[13] E. Basar, "On multiple-input multiple-output OFDM with index modulation for next generation wireless networks," *IEEE Trans. Signal Process.*, vol. 64, no. 15, pp. 3868–3878, Aug. 2016.

[14] B. Zheng, M. Wen, E. Basar, and F. Chen, "Multiple-input multiple-output OFDM with index modulation: Low-complexity detector design," *IEEE Trans. Signal Process.*, vol. 65, no. 11, pp. 2758–2772, June 2017.

[15] T. Datta, H. S. Eshwaraiah, and A. Chockalingam, "Generalized space and frequency index modulation," *IEEE Trans. Veh. Tech.*, vol. 65, no. 7, pp. 4911–4924, July 2016.

[16] T. Mao, Z. Wang, Q. Wang, S. Chen, and L. Hanzo, "Dual-mode index modulation aided OFDM," *IEEE Access*, vol. 5, pp. 50–60, Feb. 2017.

[17] M. Wen, E. Basar, Q. Li, B. Zheng, and M. Zhang, "Multiple-mode orthogonal frequency division multiplexing with index modulation," *IEEE Trans. Commun.*, vol. 65, no. 9, pp. 3892–3906, Sept. 2017.

[18] Y. Xiao, S. Wang, L. Dan, X. Lei, P. Yang, and W. Xiang, "OFDM with interleaved subcarrier-index modulation," *IEEE Commun. Lett.*, vol. 18, no. 8, pp. 1447–1450, Aug. 2014.

[19] E. Basar, "OFDM with index modulation using coordinate interleaving," *IEEE Wireless Commun. Lett.*, vol. 4, no. 4, pp. 381–384, Aug. 2015.

[20] J. Choi, "Coded OFDM-IM with transmit diversity," *IEEE Trans. Commun.*, vol. 65, no. 7, pp. 3164–3171, July 2017.

[21] M. Wen, B. Ye, E. Basar, Q. Li, and F. Ji, "Enhanced orthogonal frequency division multiplexing with index modulation," *IEEE Trans. Wireless Commun.*, vol. 16, no. 7, pp. 4786–4801, July 2017.

[22] L. Wang, Z. Chen, Z. Gong, and M. Wu, "Space-frequency coded index modulation with linear-complexity maximum likelihood receiver in MIMO-OFDM system," *IEEE Signal Process. Lett.*, vol. 23, no. 10, pp. 1439–1443, Oct. 2016.

[23] K. Fazel and S. Kaiser, *Multi-Carrier and Spread Spectrum Systems*. New York: Wiley, 2003.

[24] G. Kaddoum, Y. Nijsure, and H. Tran, "Generalized code index modulation technique for high data rate communication systems," *IEEE Trans. Veh. Tech.*, vol. 65, no. 9, pp. 7000–7009, Sept. 2016.

[25] G. Kaddoum, M. F. A. Ahmed, and Y. Nijsure, "Code index modulation: A high data rate and energy efficient communication system," *IEEE Commun. Lett.*, vol. 19, no. 2, pp. 175–178, Feb. 2015.

[26] B. M. Popovic, "Spreading sequences for multicarrier CDMA systems," *IEEE Trans. Commun.*, vol. 47, no. 6, pp. 918–926, June 1999.

[27] P. K. Frenger and N. A. B. Svensson, "Parallel combinatory OFDM signaling," *IEEE Trans. Commun.*, vol. 47, no. 4, pp. 558–567, Apr. 1999.

[28] J. Li, M. Wen, M. Zhang, and X. Cheng, "Virtual spatial modulation," *IEEE Access*, vol. 4, pp. 6929–6938, 2016.

[29] V. Tarokh, A. Naguib, N. Seshadri, and A. Calderbank, "Space-time codes for high data rate wireless communication: Performance criteria in the presence of channel estimation errors, mobility, and multiple paths," *IEEE Trans. Commun.*, vol. 47, no. 2, pp. 199–207, Feb. 1999.